Electronic Supplementary Information

Electro-synthesized Ni coordination supermolecular networks coated exfoliated graphene composite materials for high-performance asymmetric supercapacitor

Zhongheng Wang, Hua Yao, Feng Zhang, Wei Li, Yangyi Yang* and Xihong Lu

School of Materials Science and Engineering & School of Chemistry and Chemical Engineering, Sun Yat-Sen University, Xingang Xi Road No.135, Guangzhou, 510275, P.R. China

*Corresponding Author. E-mail: cesyyy@mail.sysu.edu.cn. Tel: 86-20-84112977

This file includes:

1. Figs. S1 to S15
2. References

1. Supplementary Figures

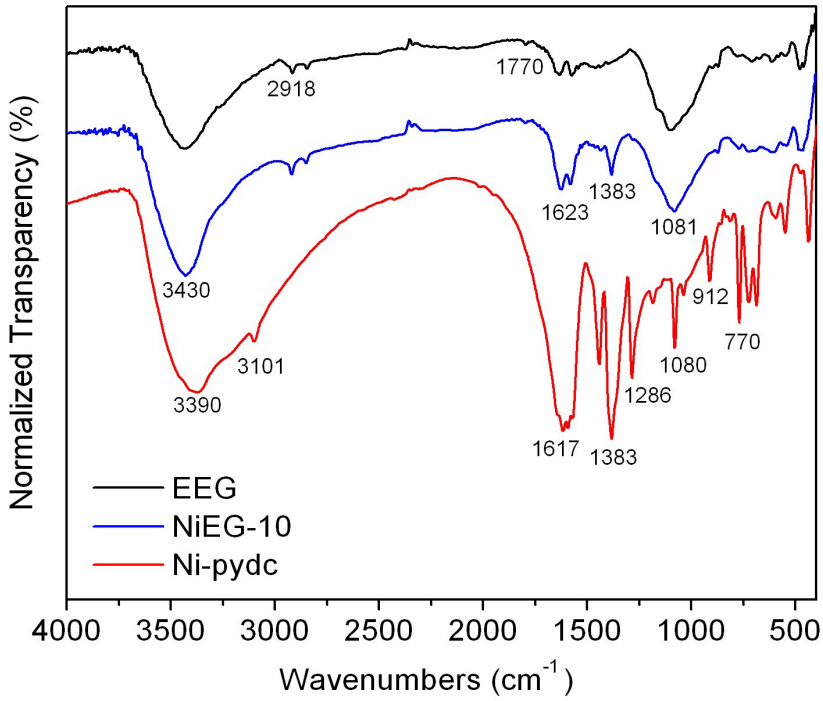

Figure S1. FT-IR spectra of the EEG/NiEG-10/Ni-pydc powder.

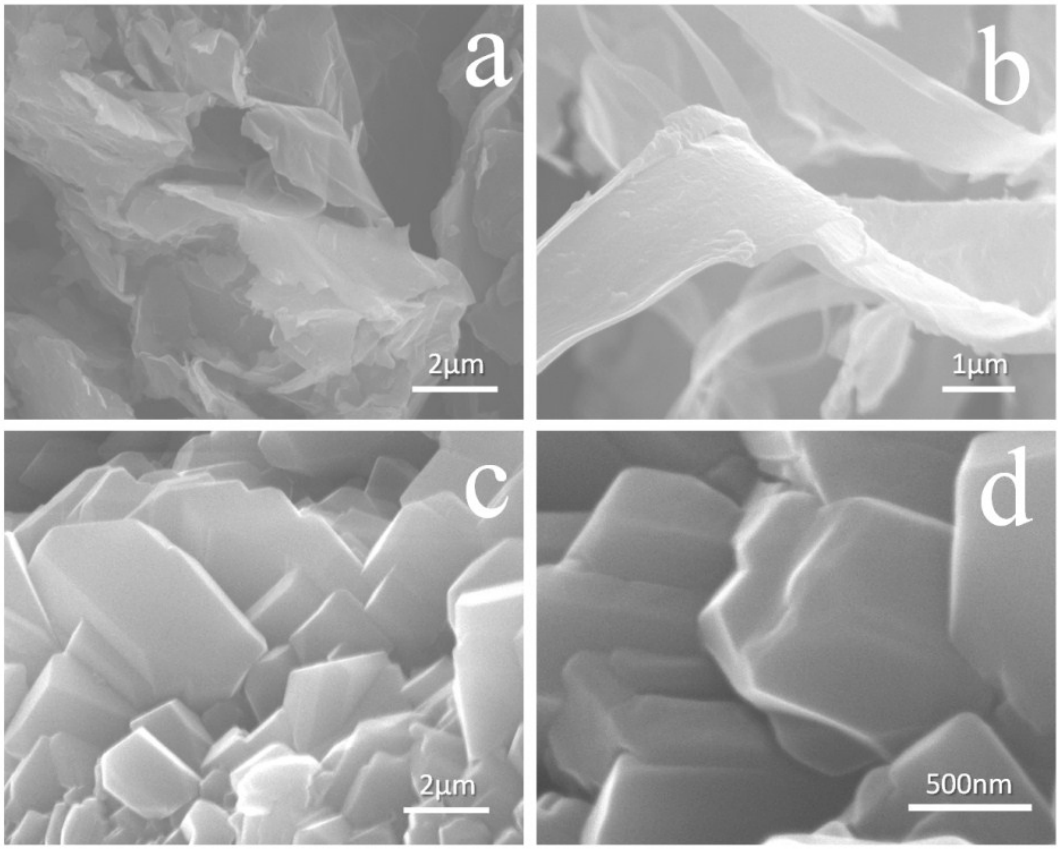

Figure S2. SEM images of the (a, b) electrochemical exfoliated graphene (EEG) flakes and (c, d) hydrothermal synthesized Ni-pydc powder.

It should be notice that the as-prepared EEG flakes have a wide range of individual difference, the size of the flakes is varying from 5 μm to 20 μm, while the thickness of these flakes is quite thin (<10 nm). SEM images of all prepared electrode samples were showed in Figure S3, following the sequence of Pure Ni-pydc to Pure EEG. The microstructures of these electrodes were quite different with each other due to the variety of Ni-pydc/EEG ratio. First, the SEM images of the pure Ni-pydc electrode showed irregular and loose bulk-shaped structures, which leads to poor charge-transfer and structural instability. With a small dosage of EEG, the NiEG-5 electrode has more firmly bulk-shaped structures, but the layers of Ni-pydc were quite dense. With a proper Ni-pydc : EEG ratio, the SEM images of NiEG-10 reveals a honeycomb-network porous structure consist of 8-20 nm Ni-pydc nanosheets evenly deposited on EEG flakes. The adherent Ni-pydc compounds bridged by π-π and lp-π interaction provided considerable pseudocapacitance with improved charge-transfer conductivity. For the EEG-rich NiEG-20 electrode, the existence of Ni-pydc network was much lesser and thinner. Since the Ni-pydc is the essential source of the pseudocapacitance of the electrode while EEG served as conductive enhancer, structural reinforce with relatively low EDLC, it's unreasonable to increase the EEG content to an unnecessary amount. As for the pure EEG electrode, the aggregation phenomenon can be clearly observed

between some EEG flakes, the light-colored pillars and nanoparticles adhere to the flakes were PVDF binder and deposited salts from the electrolyte.

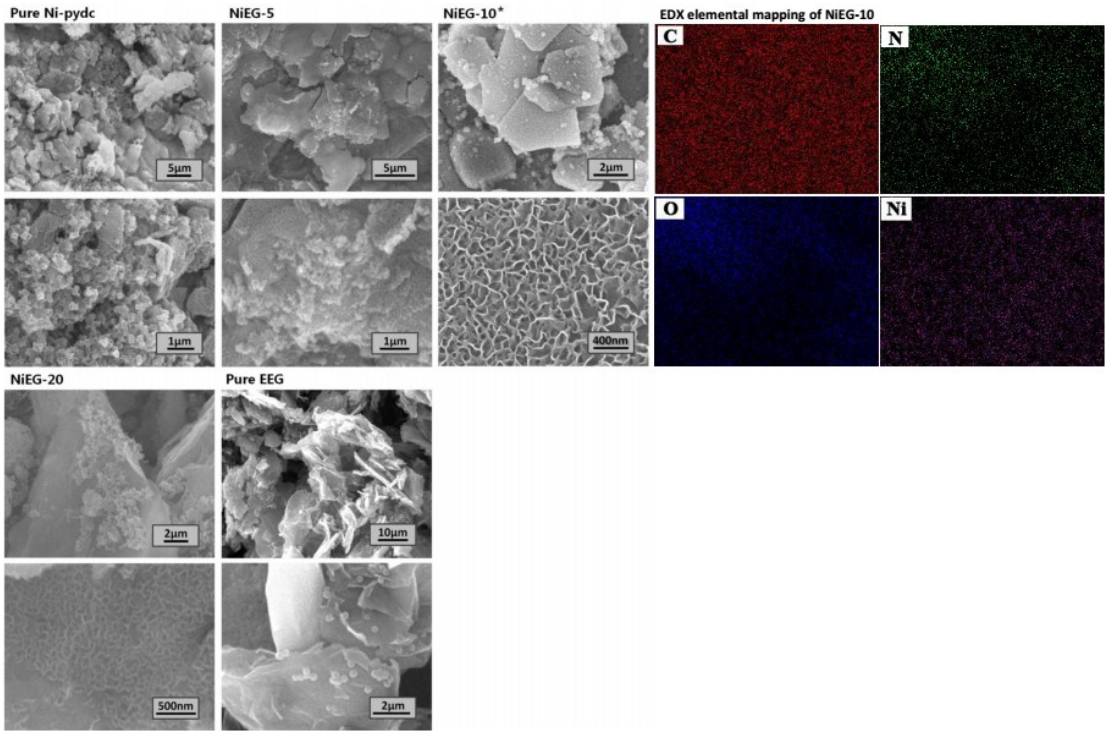

Figure S3. SEM images of a series of electrodes loaded with different active materials and a representative EDX elemental mapping of the NiEG-10 electrode.

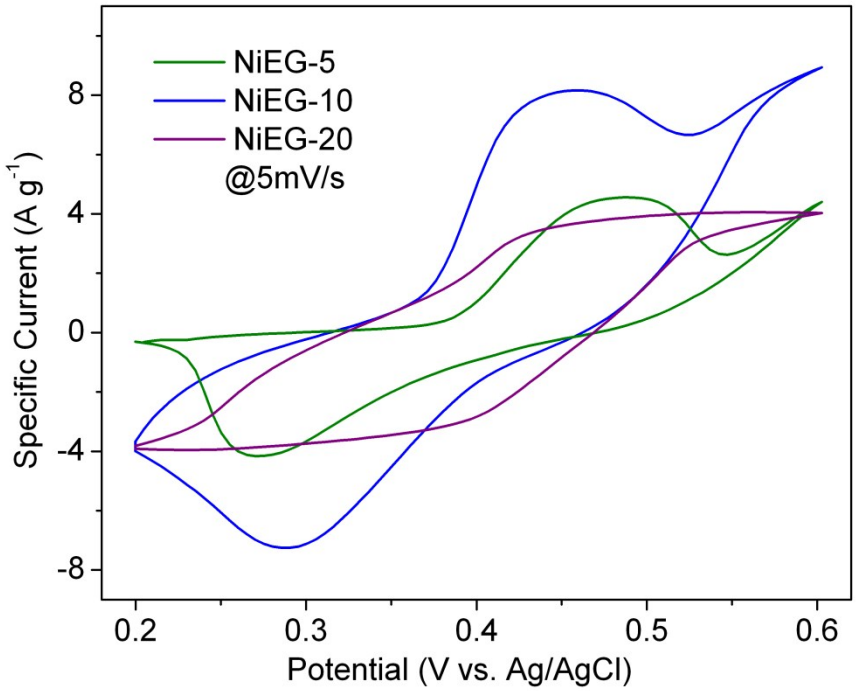

Figure S4. The CV curves of NiEG electrodes with different Ni-pydc: EEG ratio.

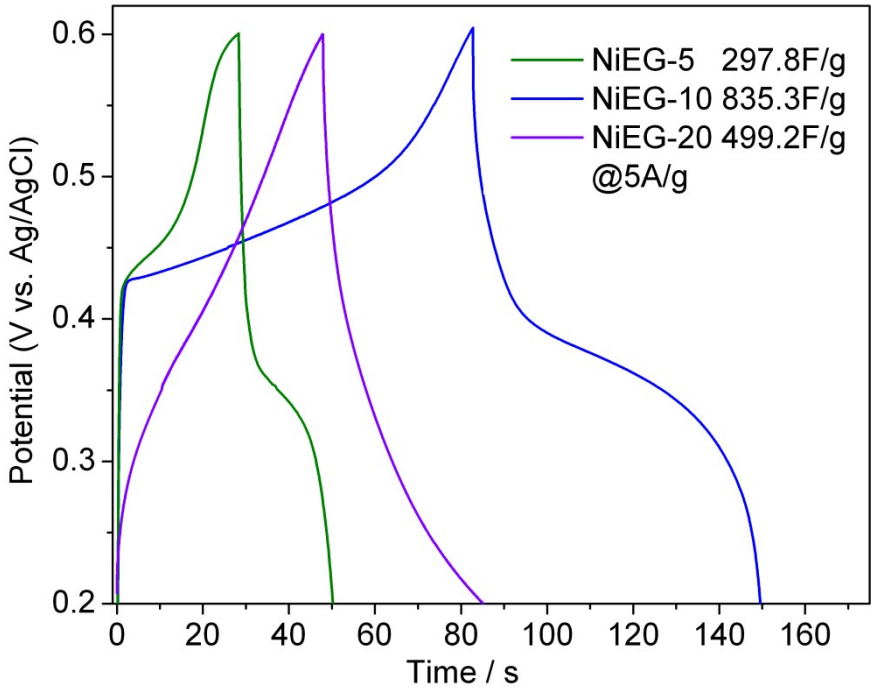

Figure S5. The GCD curves of NiEG electrodes with different Ni-pydc: EEG ratio. The specific capacitances were calculated from the discharge curves accordingly.

Table S1. The EDX elemental analysis result of NiEG-10 electrode.

Element	C	O	Ni	Au (coating)
Weight [%]	36.59	24.19	10.28	1.94
Atomic Content [%]	75.73	21.62	2.50	0.14

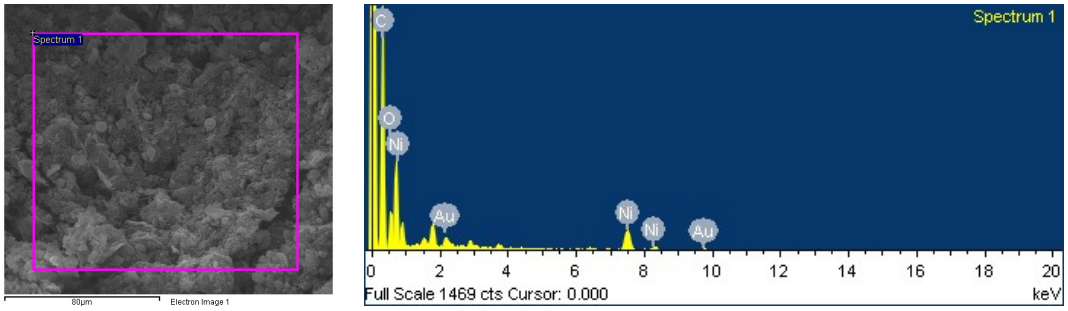

Figure S6. The energy dispersive X-ray (EDX) spectrum of the NiEG-10 electrode, the spectrum was sampled in a center hollow area (asides Ni foam frames to avoid interference from substance).

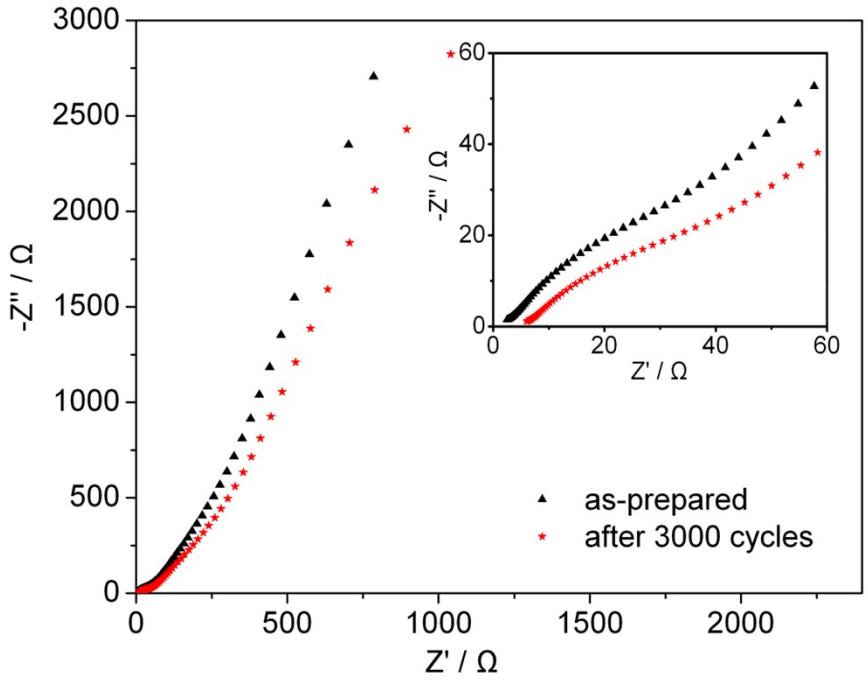

Figure S7. The EIS curves of NiEG-10 electrode before and after 3000 charge/ discharge cycles. Inserted: the enlarged view of high frequency area.

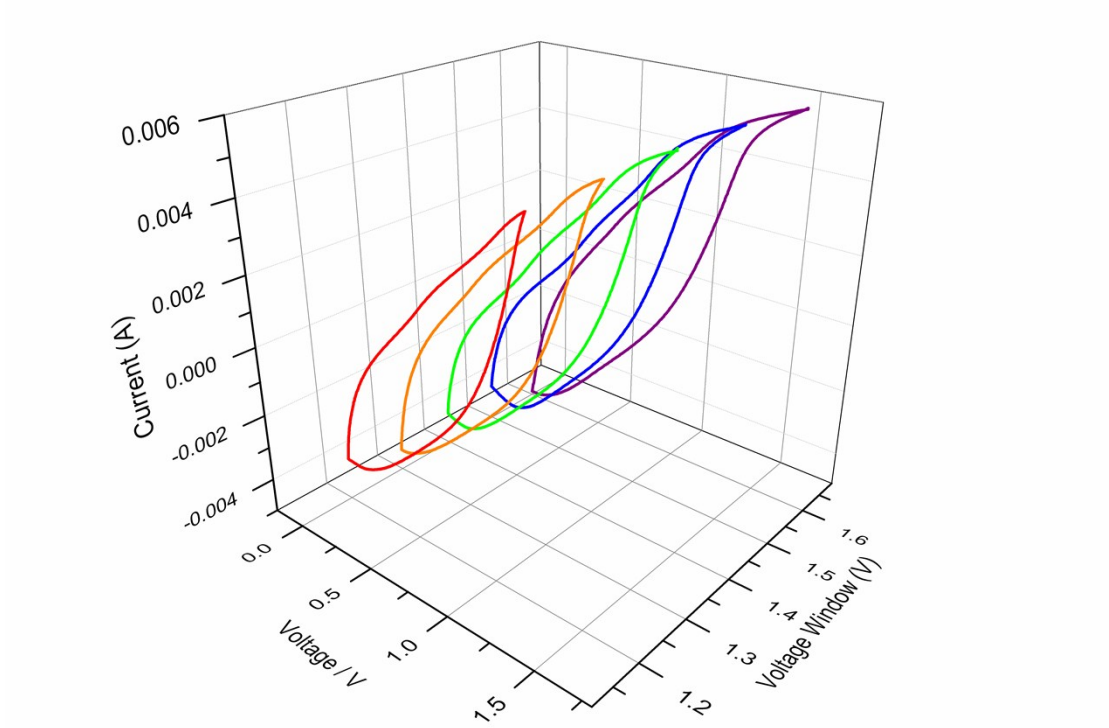

Figure S8. CV curves of the EEG//EEG SSC device in different voltage windows at 5 mv s^{-1}.

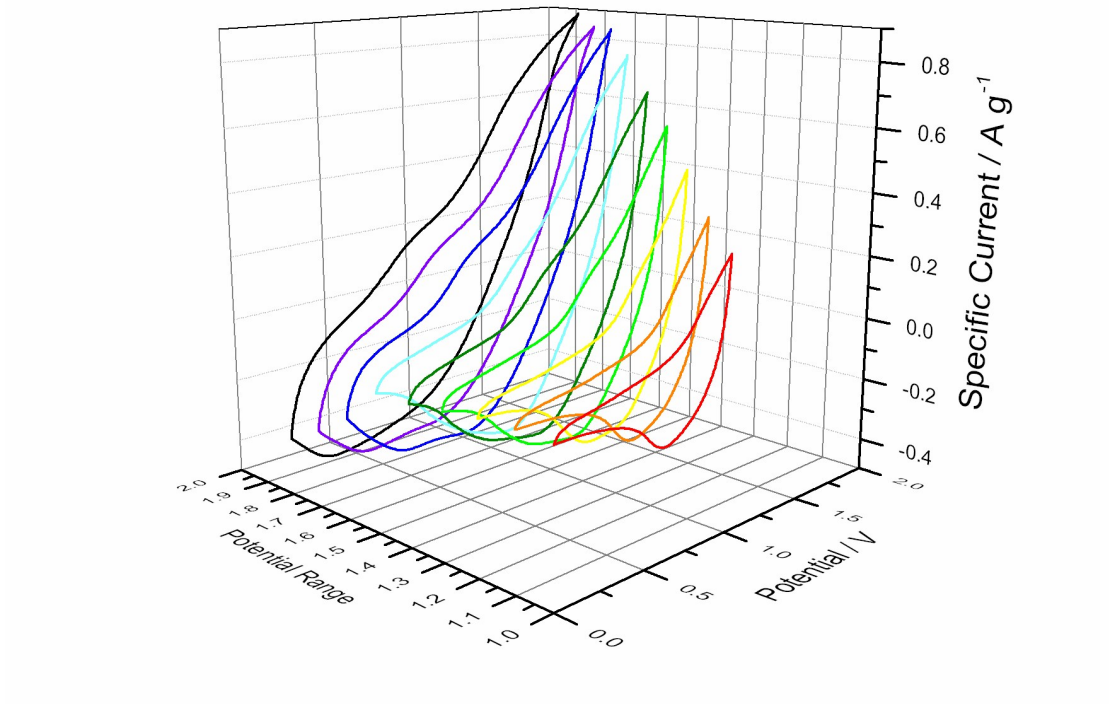

Figure S9. CV curves of the ASC device at different operating voltage windows.

Note for Figure S10

Electrochemical impedance spectroscopy (EIS) tests of the ASC device were measured from 0.01Hz to 100 kHz with amplitude of 0.05V. The EIS curve of the ASC and ideal equivalent circuit of the pseudo/EDLC hybrid ASC was shown in Fig.S10 according to the literature. [1] In this modified Randles model, the leftmost R_{Ω} represents the solution resistance resulted from ionic resistance of the electrolyte. The bottom R_{CT} and Warburg independence (Z_W) joined in series were related to the charge-transfer and faradic impedance, respectively. The C_{DL} and rightmost C_F stand for the equivalent capacitor component of the EDLC and faradic capacitor, respectively. The proposed equivalent circuit model was well fitted with the original EIS curve according to the calculated result.

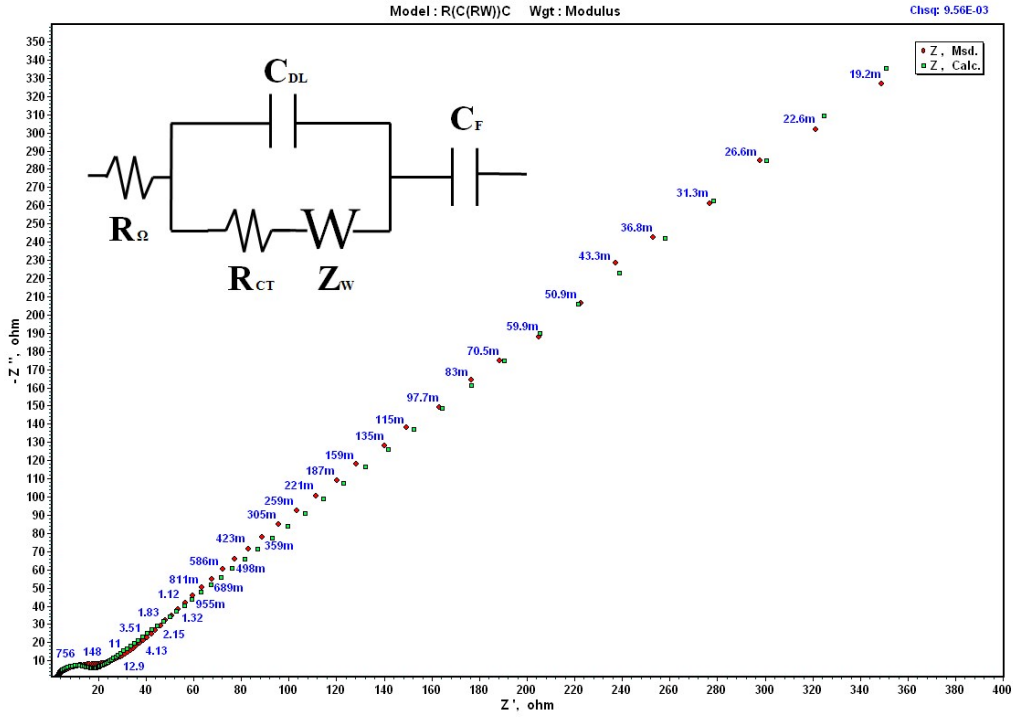

Figure S10. Measured and calculated Nyquist plot of the ASC device. (Inset: the Randles equivalent circuit model used for the calculation provided by ZSimpWin v3.20 program, Echem Software, USA).

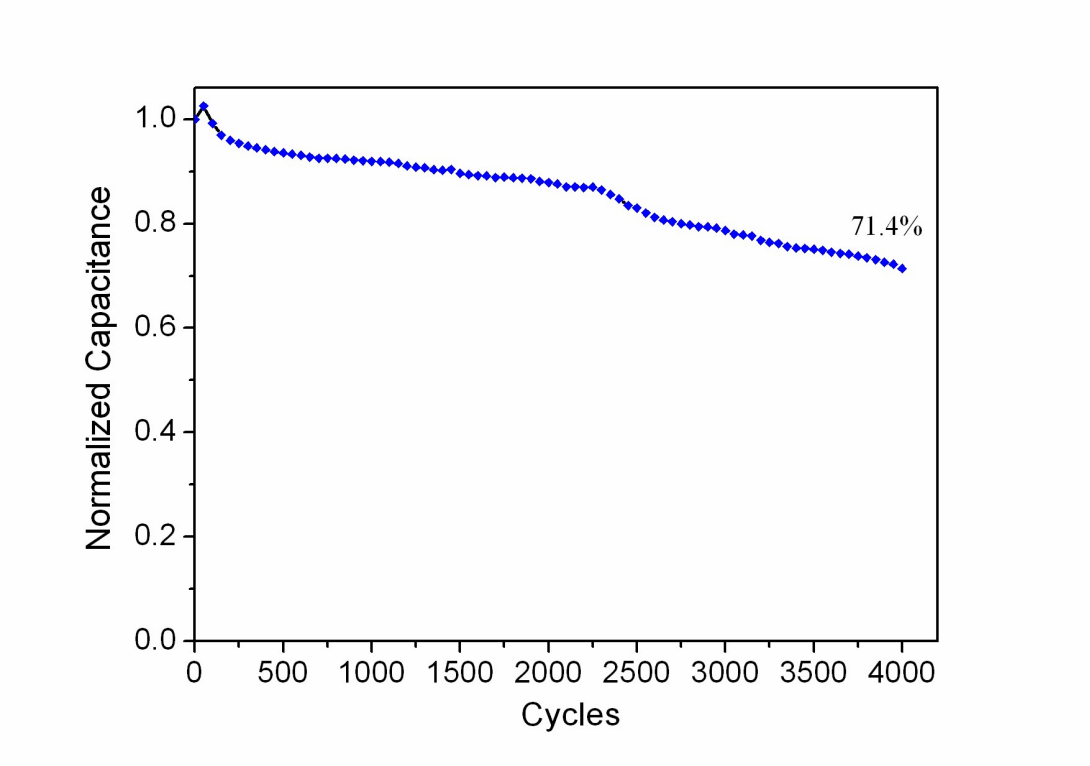

Figure S11. GCD cycling result of the ASC device at 5 A g^{-1}.

Note for Figure S12

Since the nickel foam has its own capacitance due to its porous nature and possible redox capability, [2] thus may interfere with the actual capacitance of the material. To investigating the influence of the substance, the electrochemical capacitance properties of blank nickel foam were investigated in the same condition. As illustrated in Fig. S12, the blank Ni foam shows a typical redox CV curves, probably because some Ni was oxidized during charge-discharge cycles. But the total capacitance of the blank Ni foam was far less than the NiEG-10 electrode, not to mention this extra capacitance was considered much lesser in loaded samples because the surface of Ni foam was mostly covered by the material according to SEM images. Therefore, the interference of Ni foam substrate was considered neglectable.

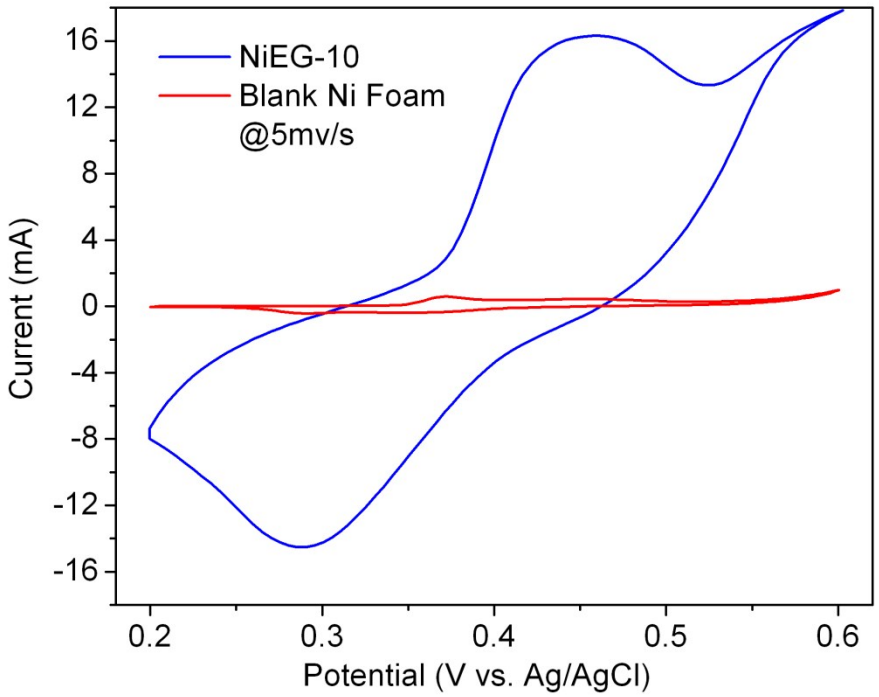

Figure S12. CV curves of NiEG-10 electrode and same-sized Ni-foam at 5 mv s^{-1}.

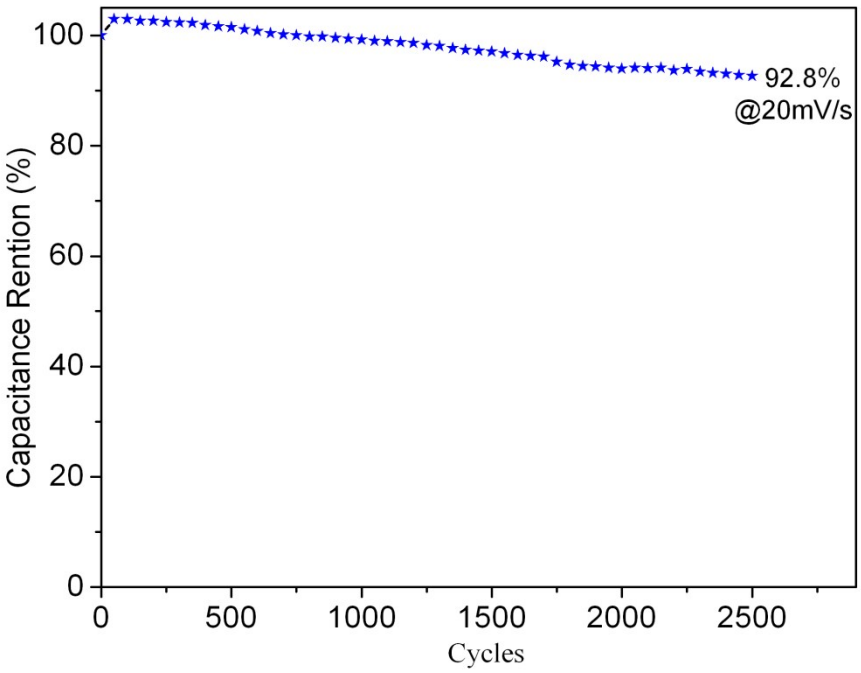

Figure S13. CV cycling result of the NiEG-10 electrode at 20 mv s^{-1}.

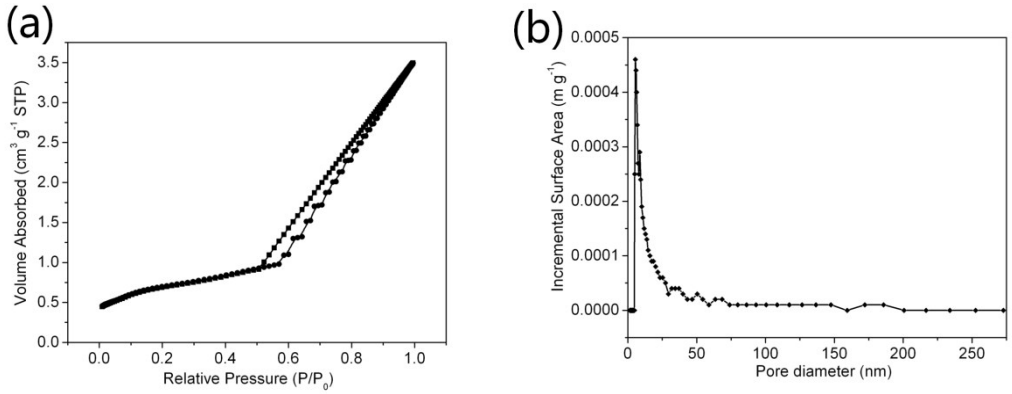

Figure S14. Nitrogen adsorption-desorption isotherms (a) and Pore size distributions (b) of as-prepared Ni-pydc powder.

Note for Figure S14 and Figure S15

Since the surface area of NiEG electrode cannot directly characterized due to instrumental limitations, the specific surface and total porous analysis of Ni-pydc powder was carried on the powder sample instead. However, the Ni-pydc powder seems changed during to the heat-treatment, the measured BET surface was quite low and the color of the powder sample was darken after 100 °C heating (Fig. S14). Furthermore, the XRD pattern of Ni-pydc powder sample after the surface analysis was quite differ with its original pattern (Fig. S15), indicated the structure collapse of Ni-

pydc supermolecular framework due to the loss of water molecule during the 150 °C pre-drying process. Because the water molecule act as essential bridge to interconnect Ni-pydc via hydrogen bonds according to the literature,[3] it's considered that the loss of water molecule will result in the decomposition of Ni-pydc framework. Therefore, the actual specific surface can't be correctly measure by common nitrogen absorption/desorption method. Since the NiEG electrode is design to working in aqueous gel environment, the heat instability over the boiling point of water is considered neglectable for practical applications.

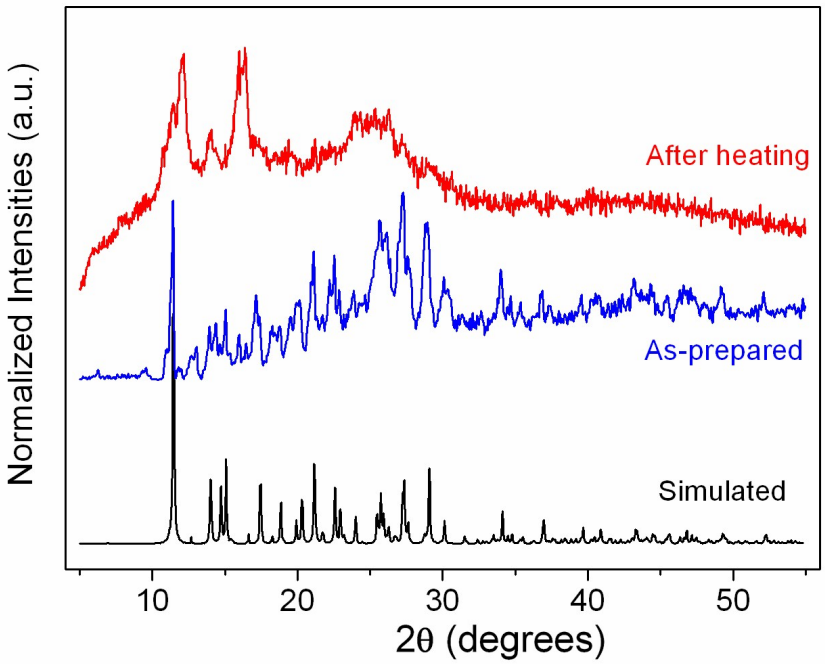

Figure S15. XRD patterns of Ni-pydc powder before and after 100 °C heating process.

2. Reference

[1] C. Kong, W. Qian, C. Zheng, Y. Yu, C. Cui and F. Wei, *Chem. Comm.* **2013**, *49*, 10727.

[2] W. Xing, S. Qiao, X. Wu, X. Gao, J. Zhou, S. Zhuo, S. B. Hartono and D. Hulicova-Jurcakova, *J. Power Sources* **2011**, *196*, 4123.

[3] M. Mirzaei, H. Eshtiagh-Hosseini, Z. Karrabi, K. Molčanov, E. Eydizadeh, J. T. Mague, A. Bauzá, A. Frontera, CrystEngComm **2014**, *16*, 5352.